Rapid Growth and Flow-Mediated Nucleation of Millimeter-Scale Aligned Carbon Nanotube Structures from a Thin-Film Catalyst

Anastasios John Hart* and Alexander H. Slocum

Department of Mechanical Engineering, Massachusetts Institute of Technology, 77 Massachusetts Avenue, Room 3-470, Cambridge, Massachusetts 02139

Received: September 27, 2005; In Final Form: February 2, 2006

We discuss the rapid growth of films and lithographically templated microstructures of vertically aligned small-diameter multiwalled carbon nanotubes (VA-MWNTs), by atmospheric-pressure thermal chemical vapor deposition (CVD) of $C_2H_4/H_2/Ar$ on a Fe/Al_2O_3 catalyst film deposited by electron beam evaporation. The structures grow to 1 mm height in 15 min and reach close to 2 mm in 60 min. The growth rate and final height of CNT microstructures grown from catalyst patterns depend strongly on the local areal density of catalyst, representing a reverse analogue of loading effects which occur in plasma etching processes. Abrupt transitions between areas of micrometer-thick tangled CNT films and millimeter-scale aligned CNT structures are manipulated by changing the duration of pretreatment by H_2/Ar prior to introduction of C_2H_4 and by changing the configuration of the substrate sample in the furnace tube. This demonstrates that the flow profile over the sample mediates the supply of reactants to the catalyst and that pretreatment using H_2 significantly affects the initial activity of the catalyst.

1. Introduction

Synthesis of macroscopic carbon nanotube (CNT) materials having mechanical, electrical, and thermal properties comparable to those of individual CNTs remains elusive, in large part due to incomplete knowledge of the growth behavior of CNTs. It is accepted that CNT growth by chemical vapor deposition (CVD) involves surface and/or bulk diffusion of carbon at a metal catalyst particle. CNT−CNT or CNT−substrate interactions in addition to the arrangement and activity of the catalytic sites determine if CNTs grow in an isolated, tangled, or aligned configuration. For example, isolated SWNTs can be grown to several millimeters or centimeters[1,2] when suspended during growth by a gas flow; however, the density of catalytic sites must be very low to prevent entanglement between CNTs. At a high catalyst density and CNT growth rate, a vertically aligned (VA) growth mode is typical whereby the CNTs self-orient perpendicular to the substrate surface due to initial crowding and continue to grow upward in this direction.[3,4] However, the mechanism of termination of vertically aligned growth is not clearly known. At all stages of CNT growth, chemical and mechanical interactions are highly coupled, and these interactions must be further understood for efficient synthesis of CNT materials containing CNTs having macroscopic lengths.

While CNT growth from floating catalytic sites[5,6] is readily more scalable for bulk synthesis, growth from substrates offers greater control of the arrangement, density, and length of CNTs. Typically, growth of aligned CNTs on a substrate is achieved using an unsaturated hydrocarbon gas such as C_2H_2[7,8] or C_2H_4[4,9] and a predeposited catalyst film or by evaporating a solution of an organometallic catalyst precursor and a liquid hydrocarbon.[10−12] Millimeter-scale architectures of aligned MWNTs have been routinely achieved using floating catalyst precursors;[13,14] however, these structures typically have lesser crystallinity and higher impurity content (e.g. metal catalyst periodically along the tube axis) than structures grown from predeposited catalyst films. Further, by adding an optimal amount of ferrocene ($Fe(C_5H_5)_2$) to C_2H_2 feedstock during growth, Eres et al.[15] increased the terminal length of VA-MWNTs, grown from a Al/Fe/Mo catalyst film, from less than 0.5 mm to greater than 3 mm. This is attributed to $Fe(C_5H_5)_2$ increasing the effectiveness of C_2H_4 by promoting its dehydrogenation before reaching the catalyst site. Further study has shown that homogeneous gas phase reactions critically affect the CNT growth process in many systems and that a minimum incidence rate of carbon-containing molecules is necessary for vertically aligned growth.[16]

Recently, the first atmospheric pressure synthesis of vertically aligned SWNTs was reported,[17] where introduction of a controlled concentration of H_2O vapor gives rapid growth of high-purity SWNT films to a thickness of up to 2.5 mm, possibly due to selective removal of catalyst-bound amorphous carbon by H_2O. Since, plasma-enhanced CVD growth of VA-SWNT[18] and VA-DWNT[19] films has been achieved without using an oxygen-containing additive.

We present growth of VA-MWNT films and microstructures from a Fe/Al_2O_3 catalyst film deposited by electron beam evaporation. The CNTs grow rapidly to at least 1 mm height when processed in $C_2H_4/H_2/Ar$ for 15 min. Incidentally, our CVD conditions are similar to those upon which the H_2O-assisted process has been studied.[17] Here, without the addition of H_2O, we synthesize thin MWNTs instead of SWNTs, yet maintain similar growth rates as the H_2O-assisted process.[20] We first studied synthesis of tangled SWNT films from $Mo/Fe/Al_2O_3$ in CH_4/H_2 and then found that the same catalyst gives poor yield of MWNTs in an otherwise identical process using C_2H_4/H_2 at 750 °C, while VA-MWNT structures grow from Fe/Al_2O_3 in C_2H_4/H_2.[21]

* Corresponding author: e-mail, ajhart@mit.edu; phone, +1-617-258-8451.

10.1021/jp055498b CCC: $33.50
Published on Web 03/11/2006

2. Materials and Methods

A catalyst film of 1.2/20 nm Fe/Al_2O_3 is deposited by electron beam evaporation in a single pump-down cycle using a Temescal VES-2550 with a FDC-8000 film deposition controller. The film thickness is measured during deposition using a quartz crystal monitor and later confirmed by Rutherford backscattering spectrometry (RBS).[22] The substrates are plain (100) 6 in. silicon wafers (p-type, 1−10 Ω cm, Silicon Quest International), which have been cleaned using a standard "piranha" (3:1 H_2SO_4/H_2O_2) solution. Because the Al_2O_3 is deposited by direct evaporation from a crucible of high-purity crystals, rather than by evaporation of Al,[9,23] or by other methods such as spin-coating of a sol−gel precursor,[24] we do not need to consider dedicated oxidation or curing steps prior to CNT growth. Catalyst patterns are fabricated by lift-off of a 1 μm layer of image-reversal photoresist (AZ-5214E): the photoresist is patterned by photolithography, catalyst is deposited over the entire wafer surface, and then the areas of catalyst on photoresist are removed by soaking in acetone for 5 min, with mild sonication.

CNT growth is performed in a single-zone atmospheric pressure quartz tube furnace (Lindberg), having an inside diameter of 22 mm and a 30 cm long heating zone, using flows of Ar (99.999%, Airgas), C_2H_4 (99.5%, Airgas), and H_2 (99.999%, BOC). The furnace temperature is ramped to the setpoint temperature in 30 min and held for an additional 15 min under 400 sccm Ar. The flows of Ar and H_2 used during growth are established typically 1−5 min prior to introducing C_2H_4, then the mixture of $C_2H_4/H_2/Ar$ is maintained for the growth period of 15−60 min. Finally, the H_2 and C_2H_4 flows are discontinued, and 400 sccm Ar is maintained for 10 min more to displace the reactant gases from the tube, before being reduced to a trickle while the furnace cools to below 100 °C.

Samples are characterized by scanning electron microscopy (SEM) using a Philips XL30-FEG-ESEM typically at 5 keV, by high-resolution transmission electron microscopy (HRTEM) using a JEOL-2010 typically at 200 keV, and by Raman spectroscopy with 647 nm excitation. TEM samples are prepared by removing a piece of the aligned CNT film with tweezers, dispersing the CNTs in methanol by vortexing for 2 min and sonicating mildly for 30 min, and air-drying a drop of the solution on a copper grid coated with a holey carbon film. For Raman spectroscopy, the microscope is focused on the sidewall of the film to maximize the G-band intensity from CNTs oriented mainly perpendicular to the laser beam. The areal density of CNTs on the substrate is calculated using the average CNT diameter measured by HRTEM imaging, the film volume which is estimated by SEM imaging, and the mass determined by scraping the film from the substrate and weighing it using a thermogravimetric analyzer (TGA, Perkin-Elmer) at room temperature.

3. Results

3.1. Thick Films and High-Aspect-Ratio Microstructures. Millimeter-tall vertically aligned CNT (VA-CNT) films are grown from the Fe/Al_2O_3 film processed in 100/500/200 sccm $C_2H_4/H_2/Ar$, at 750 °C, as shown in Figure 1. The structures grow rapidly, reaching 0.9 mm height in 15 min and terminating at 1.8 mm height after 60 min. The average growth rate of 1 μm/s during the first 15 min indicates that approximately 9300 circumferential "floors" of carbon atoms per second are added to each CNT. The side view of Figure 1b shows that the CNTs are oriented primarily perpendicular to the substrate. The CNTs are primarily arranged in strands as large as 0.1 μm diameter,

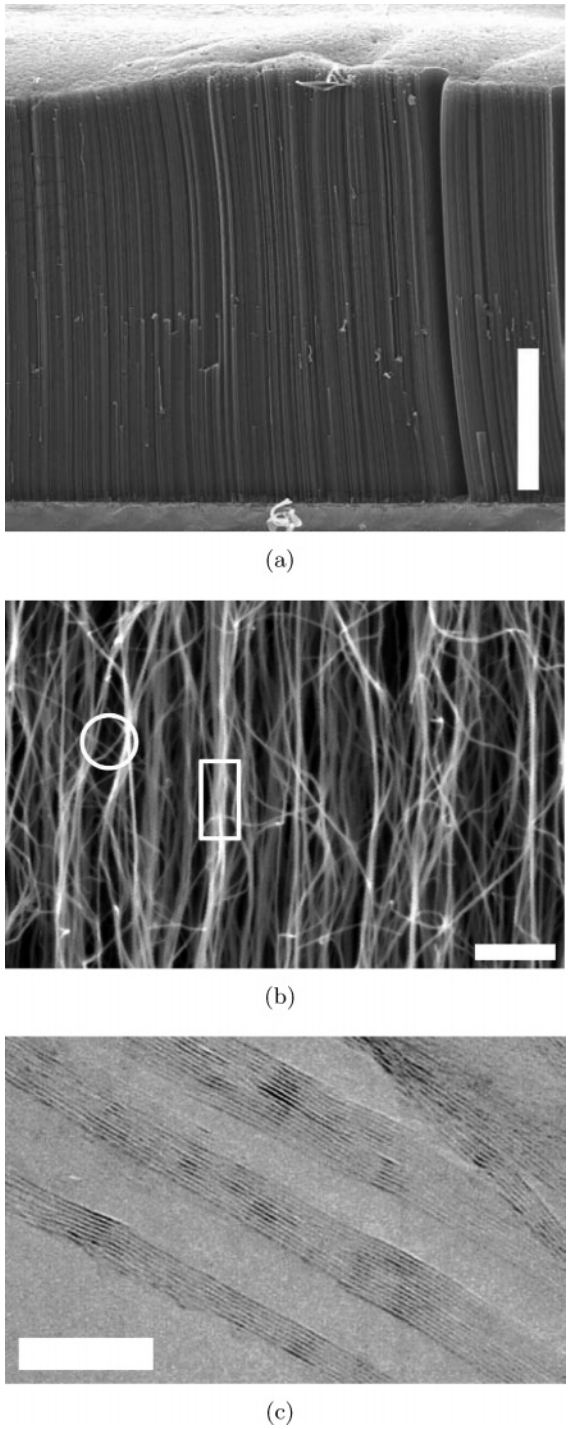

Figure 1. (a) Oblique view (stage tilted 70°) SEM image of aligned CNT film, approximately 1.8 mm high, grown in 60 min from 100/500/200 sccm $C_2H_4/H_2/Ar$ (scale 650 μm). (b) Typical alignment of CNTs within film, viewed from side (scale 0.5 μm); HRTEM images of MWNTs from film (scale 10 nm). In (b), the rectangle indicates a large strand and the circle indicates an isolated CNT bridging strands.

in which the CNTs are held closely, and there is significant bridging between nearby strands. HRTEM examination (Figure 1c) shows that the CNTs are multiwalled and tubular,[25] without bamboo-like crossovers.[26,27] The CNTs average approximately 8 nm o.d. and 5 nm i.d., and most have three to seven concentric parallel walls. By SEM examination, metal clusters are routinely observed at the roots of CNTs ripped from the substrate; however, in thorough TEM examination, we have not observed any metal particles along the CNTs. Therefore, the CNTs grow by a "base growth" mechanism,[28] where the catalyst particle

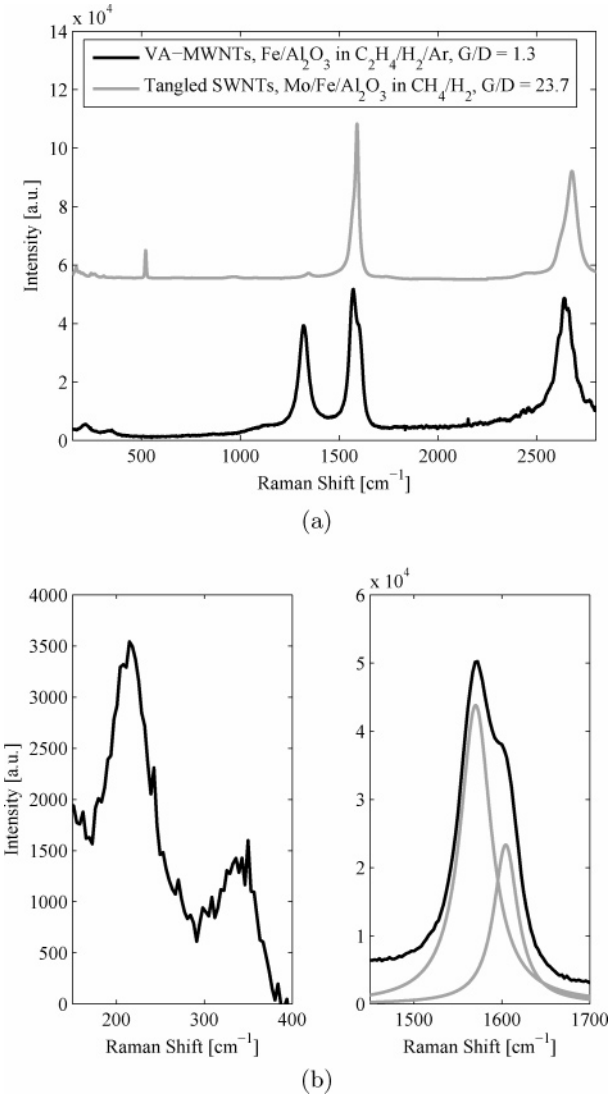

Figure 2. Typical Raman spectrum of VA-MWNT film grown at 750 °C: (a) comparison to spectrum of tangled SWNT film grown from $Mo/Fe/Al_2O_3$ in CH_4/H_2; (b) low-frequency modes (left) and Lorentzian-fit *G*-band region (right) of VA-MWNT spectrum.

remains on the substrate and new carbon is added there. The density of CNTs on the substrate is estimated as 1.5×10^{10} CNTs/cm^2 and appears the same from the top to bottom of the film sidewall, suggesting that the structures consist primarily of CNTs extending fully through the thickness.

A typical Raman spectrum (Figure 2) of our VA-MWNT films has a *G*/*D* peak intensity ratio slightly greater than unity. This is compared to the spectrum of a film of tangled SWNTs grown from a $Mo/Fe/Al_2O_3$ film in CH_4/H_2 in an identical tube furnace,[21] which has $G/D > 20$. The MWNTs also have a strong *G*′ band[29] near 2650 cm^{-1} and low-frequency modes at approximately 215 and 240 cm^{-1}. The low-frequency modes could correspond to radial breathing of inner shells of MWNTs which by the relation $d = 224/\omega_{RBM}$[30] gives $d = (1.04, 0.66)$ nm; however, by HRTEM we have not observed inner diameters smaller than 3 nm. The *G*-band is split broadly and can be decomposed into Lorentzian-shaped peaks[31] centered at 1570 and 1605 cm^{-1}.

The *G*/*D* ratio and the low-frequency modes do not change considerably through the thickness of the film (i.e., at the bottom, middle, or top of the sidewall or on the top surface which is tangled) and are not significantly affected by the position of the sample in the furnace during growth. However, the high-frequency component of the G-band is typically more prominent near the top of the film. A *G*/*D* ratio close to unity is typical for VA-MWNTs grown by other thermal CVD methods,[32,33] and the strong D-band arises from both defects in the CNTs and amorphous carbon on the sidewalls.[34] Overall, Raman characteristics of MWNTs have not yet been studied thoroughly in the literature. Additional work is needed to understand the origin of the low-frequency modes and the broad splitting of the *G*-band in our samples, as well as to characterize samples grown at a wide variety of temperatures and gas compositions.

When the catalyst film is patterned, CNT structures having identical cross sections can be grown in large arrays (Figure 3a) and complex shapes can be defined (Figure 3b). Growth depends strongly on the areal density of catalyst, as the growth rate and the final height of a CNT structure vary with its cross-sectional size and shape, and with the size and arrangement of nearby features. This is a reverse analogue to "loading" and "microloading" effects[35,36] observed in plasma etching processes, where the etch rate is affected by the local pattern density, and high-density patterns etch at a slower rate due to local depletion of etchant species. In general, for catalyst shapes having roughly equal length and width such as squares and circles, larger cross sections grow into taller CNT structures and high-density arrangements of shapes grow taller than low-density arrangements. For example, the center feature of the complex shape shown in Figure 3b grows taller than the surrounding shapes. We suspect this behavior is mediated by the local supply of active reactants to the catalyst, where larger features starve smaller features of reactants.

Significant loading effects (Figure 3e) are typically observed over 0.1−1 mm distances on the substrate and are more pronounced when a high partial flow of Ar is used. At these length scales, and among growing structures which obstruct the gas flow, gas circulation near the substrate is dominated by diffusion and natural convection. The observed loading effects further suggest that "preconditioning" the reactants by thermal and/or catalytic treatment can significantly increase CNT yield.[37−39] Accordingly, the film thickness varies by as much as an order of magnitude based on the position of the growth substrate along the hot zone of our furnace, and we find a "sweet-spot" giving the highest yield at 40−80 mm downstream from the location of the control thermocouple. We obtain maximum film thickness at the growth temperature of 750 °C. At 750 °C and 15 min growth time, the film thickness is linearly proportional to the flow of C_2H_4 for 10−75 sccm (in addition to 500/200 sccm H_2/Ar), and saturates at 75−200 sccm C_2H_4.

CNT structures having smaller cross-sectional shapes are more prone to bend and collapse during growth, particularly due to differences in growth rate across the base of the structure. As illustrated in Figure 3c, circular features wider than approximately 20 μm typically remain self-standing. The CNTs growing from the smallest features we patterned (3 μm diameter circles) are roughly aligned with one another and form single structures, which are often sharply bent and rest on the substrate. CNTs growing from even much smaller patterned areas of catalyst may not be self-aligned, as has been recently demonstrated on silica particles.[40] Oblong catalyst shapes, which grow into aligned CNT "blades", are very prone to leaning. Self-stability depends strongly on the packing density of CNTs within the aligned structure, which is related to many factors including the structure and particle density of the catalyst film, as well as the initial activity of the growth process in nucleating CNTs from the catalyst particles. However, gravitational effects are insignificant for millimeter-scale growths, as the height of CNT

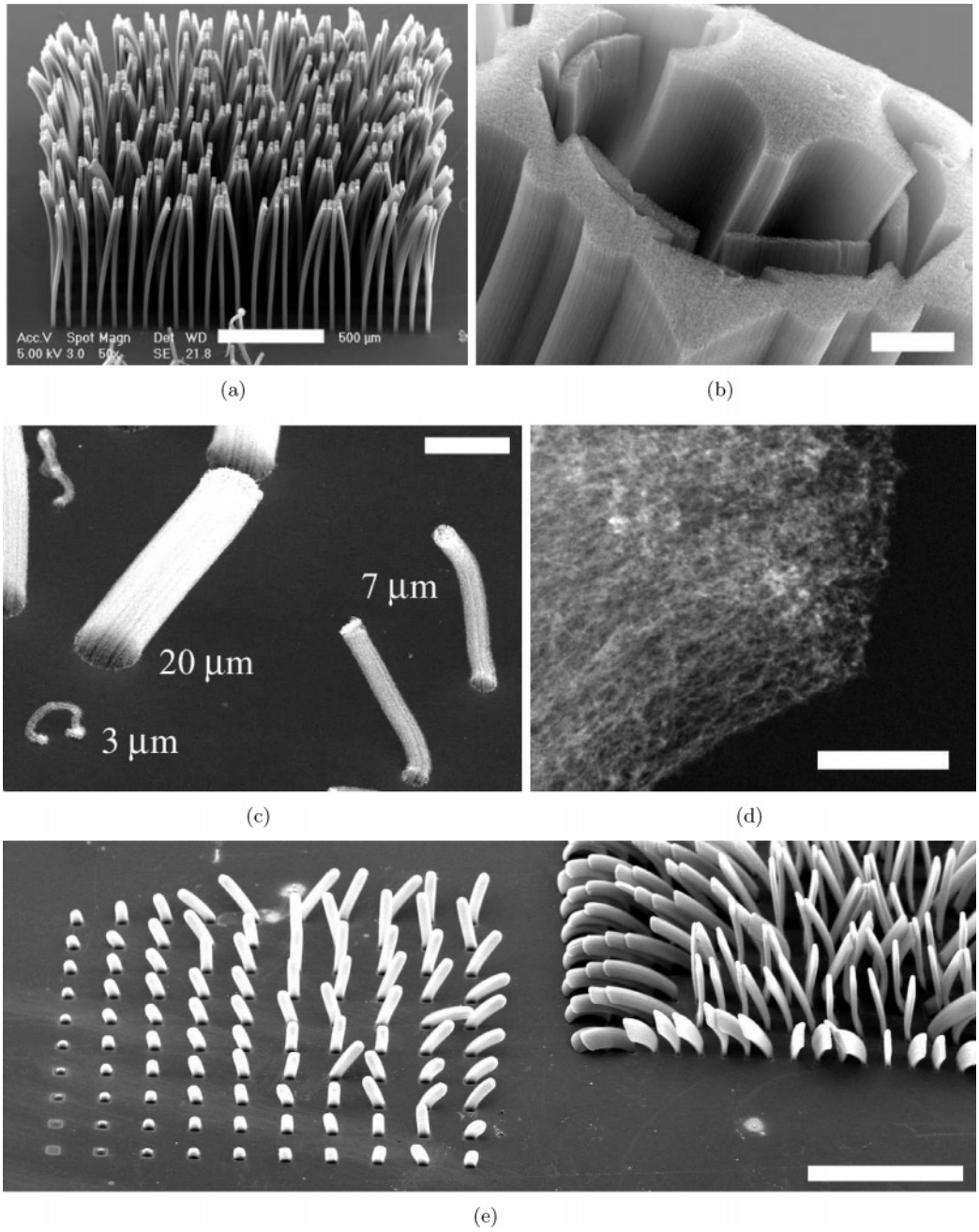

Figure 3. CNT microstructures grown from lithographically patterned catalyst: (a) array of pillars, approximately 1 mm high, grown in 15 min (scale 500 μm); (b) complex pattern which grew taller near its center, and having sharp features reproduced from high-resolution lithography mask (scale 50 μm); (c) loss of free-standing behavior as pillar diameter decreases (scale 25 μm); (d) sharp corner of patterned feature from (b) (scale 5 μm); (e) significant loading effects on pattern grown with high partial flow of Ar (scale 500 μm).

structures is no different when the substrate is inverted so the catalyst faces downward during growth.

The edges and corners of CNT structures grown from the patterned Fe/Al_2O_3 film are very sharp (Figure 3d). In our process, the sharpness is limited by the edge rounding ($R \approx 0.25\ \mu$m) of features on the laser-written lithography mask and by blurring during the exposure and development steps. However, use of higher-precision lithography for patterning the catalyst should enable CNT structures with edges which are defined by only a small number of long and parallel CNTs.

The CNT films and structures adhere weakly to the substrate and can easily be removed in bunches using tweezers or as free-standing films by gently separating the film from the substrate using a razor blade. This was also observed by Hata et al.[14] for thick films grown by the water-assisted CVD method and is desirable for applications which warrant harvesting and/or transplanting of CNTs.[41,42] On the other hand, irradiation treatment[43,44] or annealing[45] may be useful for strengthening the CNT-substrate adhesion following growth. We also observe indications of significant residual stresses in thick CNT films, which can cause delamination of the film from the substrate and may contribute to slowing or termination of growth, and are studying these effects in detail.

3.2. Flow-Mediated Growth Patterns. The pattern of VA-CNT growth depends on the placement of the substrate in the furnace and the duration of pretreatment prior to introduction of C_2H_4. We have studied these effects using the substrate configurations diagrammed in Figure 4a: "open", where the growth substrate is rested in the center of the furnace tube, 40 mm downstream of the control thermocouple; "capped", where

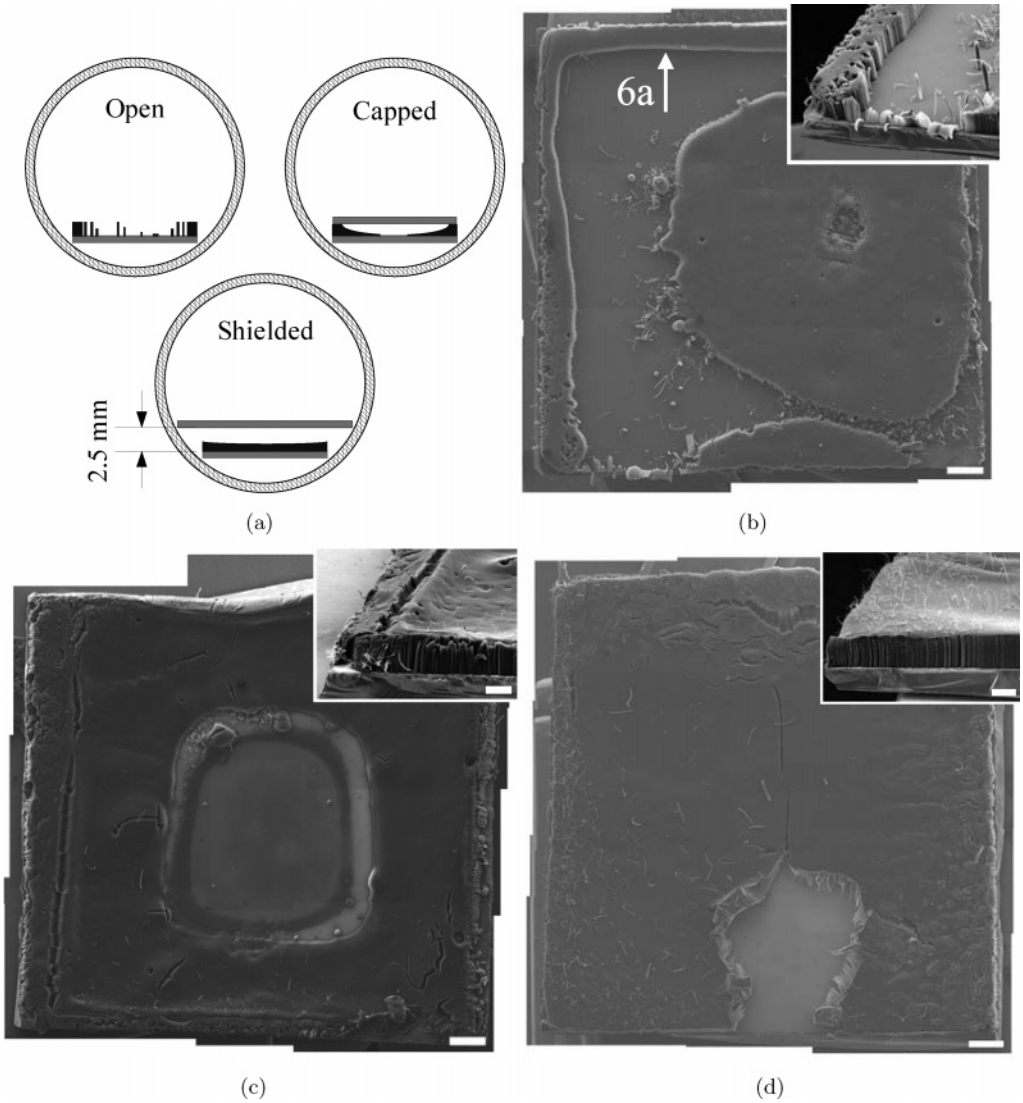

Figure 4. Substrate configurations used to establish different flow profiles over Fe/Al_2O_3-coated 15 × 15 mm silicon substrate and representations of resulting growth patterns after 1 min of pretreatment in 500/200 sccm H_2/Ar and 15 min of growth in 100/500/200 sccm C_2H_4/H_2/Ar; (b) top-view composite SEM image of sample grown in open configuration (scale 1 mm); (c) sample grown under same conditions, capped (scale 1 mm); (d) sample grown under the same conditions, shielded, with small area of film torn away by tweezers (scale 1 mm). Insets to (b−d) show oblique view SEM images of leading-edge corner of each sample (scales 0.5 mm).

a bare Si_3N_4-coated silicon substrate is placed on top of the growth substrate and held by gravity; and "shielded", where a wider Si_3N_4-coated silicon substrate is spaced above the growth substrate by approximately 2.5 mm. In the capped configuration, gas reaches the catalyst by diffusing into the gap (approximately 1 μm) between the substrates, and VA-CNT growth lifts the cap and therefore exerts a slight force. In the shielded configuration, flow proceeds through the gap and over the growth substrate at a lower velocity than in the open configuration, and flow circulation in the gap is "smoothed" by natural convection between the substrates.

When H_2 is introduced simultaneously with C_2H_4, predominately tangled (≈1 μm thick) growth occurs for all three substrate configurations, with occasional thin VA-CNT growth (≈100 μm) in the darkest areas of the photographs in Figure 5a. When H_2 is introduced 1 min in advance, thick (0.8−1.0 mm in 15 min) VA-CNT growth occurs over larger areas. The open substrate (Figure 4b) has aligned growth primarily around the periphery, with abrupt transitions (Figure 6a) between the aligned and tangled regions. The capped substrate (Figure 4b) has aligned growth around the periphery, with gradually decreasing thickness leading to a tangled region in the center area. The shielded substrate (Figure 4b) is fully covered with VA-CNTs. For 2.5 and 5 min of pretreatment (parts b and c of Figure 5), the open and shielded substrates are fully covered with thick VA-CNTs, and the capped substrate shows increased VA-CNT coverage toward the center area. In all 1−5 min cases, the film thickness on the shielded substrate is more uniform than that on the open substrate, owing to the smooth gas flow pattern over the growth substrate. For pretreatment exceeding 5 min, VA-CNT coverage decreases, and occurs primarily at the periphery of the substrates as well as in circular pillars at the center areas. This is shown for 15 min pretreatment in Figure 5d.

4. Discussion

When CNT growth begins, a vertically aligned morphology emerges if there is a sufficient density of growing CNTs to cause crowding. The growth sites must be chemically active, and there must be a sufficient carbon supply to feed all the sites simultaneously. If alignment is not achieved, tangled growth terminates shortly because of steric hindrance among the CNTs.

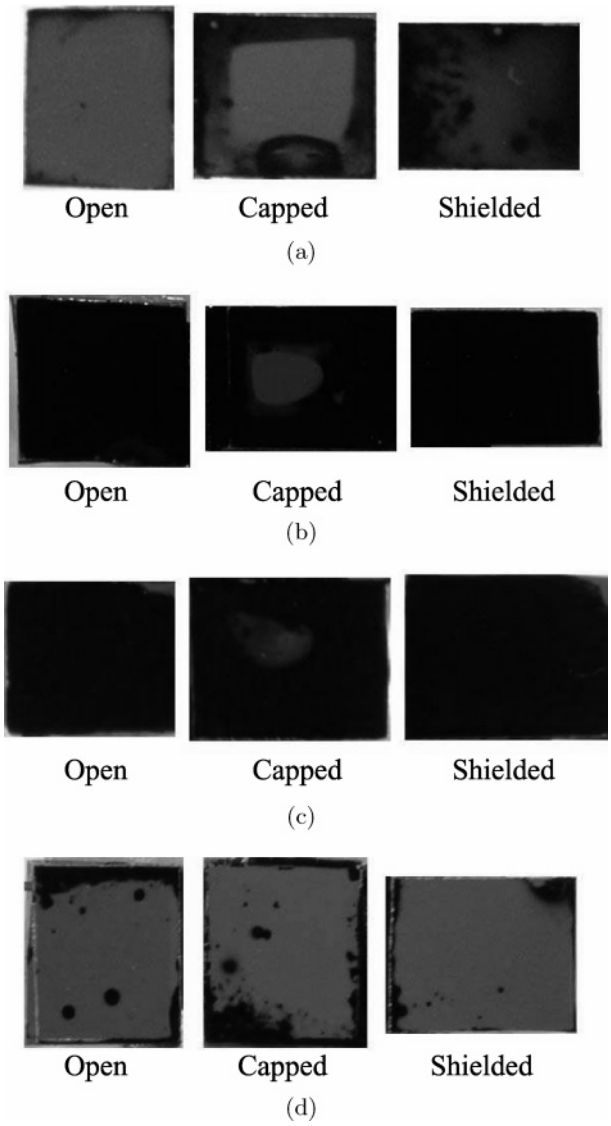

Figure 5. Optical top-view images of samples grown in open, capped, and shielded configurations, with different durations of H_2/Ar pretreatment prior to introduction of C_2H_4: (a) 0; (b) 2.5; (c) 5; (d) 15 min.

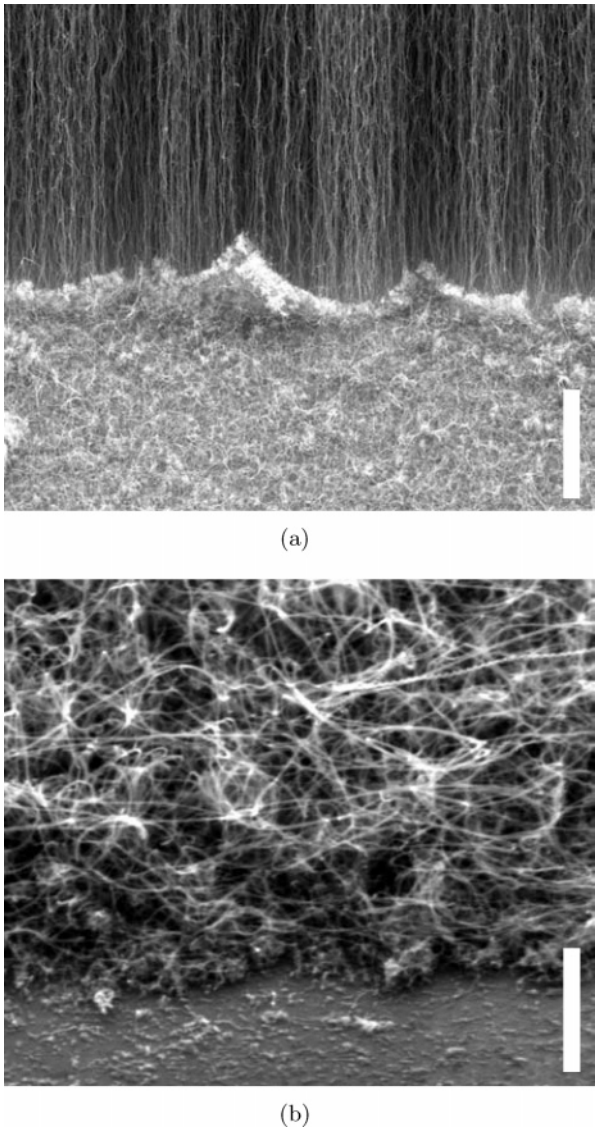

Figure 6. (a) Abrupt transition between tangled and vertically aligned growth regions, on open sample with viewing angle indicated by arrow in Figure 4b (scale 5 μm); (b) Tangled region, where film has been scratched with tweezers (in lower portion of image) to reveal thickness of approximately 1 μm (scale 1 μm).

The supply of gas to the catalyst is affected by the flow circulation within the boundary layer over the substrate, and the shape of flow field around the substrate affects the pattern of growth because rapid growth of a VA-CNT film converts a large quantity of gaseous carbon into solid carbon. For example, assuming a 1% conversion rate of the hydrocarbon source, growth of VA-MWNTs (1% areal coverage, 5 walls per CNT) at 60 μm/min. requires approximately 16 sccm C_2H_4, while growth of 1 cm^2 of tangled SWNTs (0.1% areal activity of catalyst film) at 1 μm/min requires approximately 0.35 sccm CH_4. In the latter case, the CNT growth rate is easily limited by the reaction rate at the catalyst particle and uniformity of growth is relatively unaffected by the flow profile around the substrate; in the former case, the conversion rate is a substantial fraction of the total carbon supply flowing through the furnace, and therefore spatial and temporal nonuniformities in the flow directly affect the growth pattern in areas where the catalyst does not receive enough feedstock. Continuous spatial gradients in the rate of carbon supply to the catalyst result in nearly discrete spatial transitions from tangled to aligned growth.

Therefore, as observed on the open substrate with 1 min H_2 pretreatment, areas in the "wake" of the leading edge do not receive a sufficient supply of active carbon species, leading to tangled growth in these areas. On capped substrates, gaseous carbon is consumed by the VA-CNT growth reaction around the periphery, and tangled growth occurs in the center area because the gas is restricted from and/or consumed before reaching the center area. For a given substrate size, the flow field around the substrate is relatively independent of the gas mixture, so changing the mixture to increase the concentration of active carbon species also increases the area on which vertical growth is active. However, once VA-CNT growth is established, it can proceed in a lesser supply of active species than is necessary for initiation.

It is evident that pretreatment increases the initial conversion rate of hydrocarbon to CNTs on the substrate, so areas receiving relatively less circulation of C_2H_4 at the start of the growth period are activated in the VA-CNT mode. Generally, H_2 can increase the activity of metal catalysts for cracking hydrocarbons, as well as "clean" catalytic surfaces by etching polycyclic hydrocarbon species which tend to encapsulate metal surfaces.[46,47] Reduction of the catalyst to metallic Fe by H_2 may

promote improved CNT nucleation,[48] yet prolonged treatment with H_2 may suppress growth by causing sintering of metal particles or altering metal−support interactions.[49]

Further, synergy between the metal catalyst and the supporting material is critical for an efficient and high-yield CVD growth process. CNT growth from Al_2O_3-supported catalysts has been studied widely,[24,50] and the enhanced catalytic activity of a metal nanoparticle is attributed to many effects including strong dispersion, enhanced electron transfer, high surface roughness, and enhanced decomposition of hydrocarbons on the Al_2O_3 surface.[51−55] In our process, Fe-coated SiO_2 substrates give only occasional areas of aligned CNTs, and Fe-coated bare Si substrates give no aligned CNTs and only sparse tangled and highly defective CNTs. However, aligned CNTs grow at high yields on Fe/Al_2O_3 substrates we prepare by a variety of methods, and process under identical CVD conditions as the Fe/Al_2O_3 film on Si. For example, CNT films exceeding 500 μm thick grow in 15 min on Si substrates which are coated with 10 nm Al_2O_3 by e-beam evaporation and then soaked in 0.01 M $Fe(NO_3)_3$ in 2-propanol for 5 min and dried in ambient air. Aligned CNTs grow radially from 20 μm diameter Al_2O_3 fibers cut from a cloth (McMaster-Carr), which is similarly loaded with Fe by soaking in the $Fe(NO_3)_3$ solution. We also note that millimeter-high VA-CNTs are grown from Fe/Al_2O_3 films which are rapidly heated to the growth temperature in only 1−2 min, indicating that the normal 30−45 min heating and annealing duration is not needed to form nanoparticles from the physically deposited catalyst film. Among all cases, the products are MWNTs having comparable diameters and crystallinity which grow as rapidly as 1 μm/s on average.

5. Conclusion

Rapid growth of millimeter-scale vertically aligned films and patterned microstructures of small-diameter MWNTs is achieved by simple atmospheric-pressure thermal CVD of C_2H_4. The structures grow to 1 mm height in 15 min at 750°C, and reach close to 2 mm in 60 min, from a single layer of Fe/Al_2O_3 deposited on polished Si by e-beam evaporation. Direct control of the transition between a tangled and aligned morphology is achieved by briefly pretreating the sample with H_2/Ar at the growth temperature and by changing the flow distribution around the sample. Further, area-dependent loading effects on growth from lithographically patterned catalysts suggest the importance of preconditioning the reactant mixture by controlling the flow over the catalyst. Overall, for efficient synthesis of extended-length CNT strands, growth systems must maintain spatial uniformity and temporal control of chemical and mechanical conditions at the catalyst surface and among growing CNTs.

Acknowledgment. This work was funded by NSF Grant No. DMI-0521985 and by an Ignition Grant from the MIT Deshpande Center for Technological Innovation. A. J. Hart is grateful for a Fannie and John Hertz Foundation Fellowship. Thanks to Y. M. Chiang for use of his laboratory space, S. Bhaviripudi and R. Bennett for HRTEM imaging, H. Son for assistance with and discussions regarding Raman spectroscopy, and H. Taylor for discussions regarding loading effects.

References and Notes

(1) Huang, S. M.; Cai, X. Y.; Liu, J. *J. Am. Chem. Soc.* **2003**, *125*, 5636−5637.
(2) Zheng, L. *Nat. Mater.* **2004**, *3*, 673−676.
(3) Terrones, M.; Grobert, N.; Olivares, J.; Zhang, J. P.; Terrones, H.; Kordatos, K.; Hsu, W. K.;Hare, J. P.; Townsend, P. D.; Prassides, K.; Cheetham, A. K.; Kroto, H. W.; Walton, D. R. M. *Nature* **1997**, *388*, 52−55.
(4) Fan, S. S.; Chapline, M. G.; Franklin, N. R.; Tombler, T. W.; Cassell, A. M.; Dai, H. J. *Science* **1999**, *283*, 512−514.
(5) Endo, M. *CHEMTECH* **1988**, *18*, 568−576.
(6) Li, Y. L.; Kinloch, I. A.; Windle, A. H. *Science* **2004**, *304*, 276−278.
(7) Pan, Z. W.; Xie, S. S.; Chang, B. H.; Wang, C. Y.; Lu, L.; Liu, W.; Zhou, M. Y.; Li, W. Z. *Nature* **1998**, *394*, 631−632.
(8) Cui, H.; Eres, G.; Howe, J. Y.; Puretkzy, A.; Varela, M.; Geohegan, D. B.; Lowndes, D. H. *Chem. Phys. Lett.* **2003**, *374*, 222−228.
(9) Delzeit, L.; Nguyen, C. V.; Chen, B.; Stevens, R.; Cassell, A.; Han, J.; Meyyappan, M. *J. Phys. Chem. B* **2002**, *106*, 5629−5635.
(10) Rao, C. N. R.; Sen, R.; Satishkumar, B. C.; Govindaraj, A. *Chem. Commun.* **1998**, 1525−1526.
(11) Zhang, Z. J.; Wei, B. Q.; Ramanath, G.; Ajayan, P. M. *Appl. Phys. Lett.* **2000**, *77*, 3764−3766.
(12) Singh, C.; Shaffer, M. S. P.; Koziol, K. K. K.; Kinloch, I. A.; Windle, A. H. *Chem. Phys. Lett.* **2003**, *372*, 860−865.
(13) Lee, C. J.; Lyu, S. C.; Kim, H. W.; Park, C. Y.; Yang, C. W. *Chem. Phys. Lett.* **2002**, *359*, 109−114.
(14) Deck, C.; Vecchio, K. *J. Phys. Chem. B* **2005**, *109*, 12353−12357.
(15) Eres, G.; Puretzky, A. A.; Geohegan, D. B.; Cui, H. *Appl. Phys. Lett.* **2004**, *84*, 1759−1761.
(16) Eres, G.; Kinkhabwala, A. A.; Cui, H.; Geohegan, D. B.; Puretkzy, A. A.; Lowndes, D. H. *J. Phys. Chem. B* **2005**, *109*, 16684−16694.
(17) Hata, K.; Futaba, D. N.; Mizuno, K.; Namai, T.; Yumura, M.; Iijima, S. *Science* **2004**, *306*, 1362−1364.
(18) Zhong, G.; Iwasaki, T.; Honda, K.; Ohdomari, I.; Kawarada, H. *Chem. Vap. Deposition* **2005**, *11*, 127−130.
(19) Hiramatsu, M.; Nagao, H.; Taniguchi, M.; Amano, H.; Ando, Y.; Hori, M. *Jpn. J. Appl. Phys.* **2005**, *44*, L693−L695.
(20) Futaba, D.; Hata, K.; Yamada, T.; Mizuno, K.; Yumura, M.; Iijima, S. *Phys. Rev. Lett.* **2005**, 95.
(21) Hart, A. J.; Slocum, A. H.; Royer, L. *Carbon* **2006**, *44*, 348−359.
(22) Chu, W. K.; Mayer, J. W.; Nicolet, M. A. *Backscattering spectrometry*; Academic Press: New York, 1978.
(23) de los Arcos, T.; Garnier, M. G.; Oelhafen, P.; Mathys, D.; Seo, J. W.; Domingo, C.;Garci-Ramos, J. V.; Sanchez-Cortes, S. *Carbon* **2004**, *42*, 187−190.
(24) Ward, J. W.; Wei, B. Q.; Ajayan, P. M. *Chem. Phys. Lett.* **2003**, *376*, 717−725.
(25) Kayastha, V. K.; Yap, Y. K.; Pan, Z.; Ivanov, I. N.; Puretzky, A. A.; Geohegan, D. B. *Appl. Phys. Lett.* **2005**, *86*, 253105.
(26) Lee, C. J.; Park, J. *J. Phys. Chem. B* **2001**, *105*, 2365−2368.
(27) Lee, Y. T.; Park, J.; Choi, Y. S.; Ryu, H.; Lee, H. J. *J. Phys. Chem. B* **2002**, *106*, 7614−7618.
(28) Dresselhaus, M. S.; Dresselhaus, G.; Avouris, P. *Carbon nanotubes: synthesis, structure, properties, and applications*; Springer: New York, 2001; Vol. 80.
(29) Shimada, T.; Sugai, T.; Fantini, C.; Souza, M.; Cancado, L. G.; Jorio, A.; Pimenta, M. A.; Salto, R.; Gruneis, A.; Dresselhaus, G.; Dresselhaus, M. S.; Ohno, Y.; Mizutani, T.; Shinohara, H. *Carbon* **2005**, *43*, 1049−1054.
(30) Bandow, S.; Asaka, S.; Saito, Y.; Rao, A. M.; Grigorian, L.; Richter, E.; Eklund, P. C. *Phys. Rev. Lett.* **1998**, *80*, 3779−3782.
(31) Jorio, A.; Pimenta, M. A.; Souza, A. G.; Saito, R.; Dresselhaus, G.; Dresselhaus, M. S. *New J. Phys.* **2003**, *5*, 139.1−139.17.
(32) Puretzky, A. A.; Geohegan, D. B.; Jesse, S.; Ivanov, I. N.; Eres, G. *Appl. Phys. A* **2005**, *81*, 223−240.
(33) Kim, K. E.; Kim, K. J.; Jung, W. S.; Bae, S. Y.; Park, J.; Choi, J.; Choo, J. *Chem. Phys. Lett.* **2005**, *401*, 459−464.
(34) Dillon, A.; Parilla, P.; Alleman, J.; Gennett, T.; Jones, K.; Heben, M. *Chem. Phys. Lett.* **2005**, *401*, 522−528.
(35) Hedlund, C.; Blom, H. O.; Berg, S. *J. Vacuum Sci. Technol., A* **1994**, *12*, 1962−1965.
(36) Karttunen, J.; Kiihamaki, J.; Franssila, S. Loading effects in deep silicon etching. In *Micromachining and Microfabrication Process Technology VI*; SPIE: Bellingham, WA, 2000; Vol. 4174.
(37) Franklin, N. R.; Dai, H. J. *Adv. Mater.* **2000**, *12*, 890−894.
(38) Endo, M.; Muramatsu, H.; Hayashi, T.; Kim, Y. A.; Terrones, M.; Dresselhaus, M. *Nature* **2005**, *433*, 476.
(39) Muramatsu, H.; Hayashi, T.; Kim, Y. A.; Endo, M.; Terrones, M.; Dresselhaus, M. S. *J. Nanosci. Nanotechnol.* **2005**, *5*, 404−408.
(40) Agrawal, S.; Kumar, A.; Frederick, M. J.; Ramanath, G. *Small* **2005**, *1*, 823−826.
(41) El-Aguizy, T. A.; Jeong, J. H.; Jeon, Y. B.; Li, W. Z.; Ren, Z. F.; Kim, S. G. *Appl. Phys. Lett.* **2004**, *85*, 5995−5997.
(42) Jeong, T.; Heo, J.; Lee, J.; Lee, S.; Kim, W.; Lee, H.; Park, S.; Kim, J. M.; Oh, T.; Park, C.; Yoo, J. B.; Gong, B.; Lee, N.; Yu, S. *Appl. Phys. Lett.* **2005**, 87.
(43) Imholt, T. J.; Dyke, C. A.; Hasslacher, B.; Perez, J. M.; Price, D. W.; Roberts, J. A.;Scott, J. B.; Wadhawan, A.; Ye, Z.; Tour, J. M. *Chem. Mater.* **2003**, *15*, 3969−3970.

(44) Krasheninnikov, A. V.; Nordlund, K. *Nucl. Instrum. Methods Phys. Res., Sect. B* **2004**, *216*, 355−366.
(45) Cao, A.; Veedu, V. P.; Li, X.; Yao, Z.; Ghasemi-Nejhad, M. N.; Ajayan, P. M. *Nat. Mater.* **2005**, *4*, 540−545.
(46) La Cava, A. I.; Bernardo, C. A.; Trimm, D. L. *Carbon* **1982**, *20*, 219−223.
(47) Jablonski, G. A.; Geurts, F. W.; Sacco, A.; Biederman, R. R. *Carbon* **1992**, *30*, 87−98.
(48) Nishimura, K.; Okazaki, N.; Pan, L. J.; Nakayama, Y. *Jpn. J. Appl. Phys.* **2004**, *43*, L471−L474.
(49) Ago, H.; Nakamura, K.; Uehara, N.; Tsuji, M. *J. Phys. Chem. B* **2004**, *108*, 18908−18915.
(50) Kong, J.; Soh, H. T.; Cassell, A. M.; Quate, C. F.; Dai, H. J. *Nature* **1998**, *395*, 878−881.
(51) Vander Wal, R. L.; Ticich, T. M.; Curtis, V. E. *Carbon* **2001**, *39*, 2277−2289.
(52) de los Arcos, T.; Garnier, M. G.; Seo, J. W.; Oelhafen, P.; Thommen, V.; Mathys, D. *J. Phys. Chem. B* **2004**, *108*, 7728−7734.
(53) Dai, H. J.; Kong, J.; Zhou, C. W.; Franklin, N.; Tombler, T.; Cassell, A.; Fan, S. S.;Chapline, M. *J. Phys. Chem. B* **1999**, *103*, 11246−11255.
(54) Seidel, R.; Duesberg, G. S.; Unger, E.; Graham, A. P.; Liebau, M.; Kreupl, F. *J. Phys. Chem. B* **2004**, *108*, 1888−1893.
(55) Vasileva, N. A.; Buyanov, R. A.; Klimik, I. N. *Kinet. Catal.* **1980**, *21*, 175−179.